

Evaluation of cavity quantum electrodynamics parameters for a planar-cavity geometry

Kazuki Koshino*

*Faculty of Systems Engineering, Wakayama University, 930 Sakaedani Wakayama 640-8510, Japan
and CREST, Japan Science and Technology Agency, 4-1-8 Honcho, Kawaguchi, Saitama 332-0012, Japan*

(Received 9 September 2005; published 15 May 2006)

We investigate how a two-level system inside of a planar cavity behaves as a cavity quantum electrodynamics (QED) system. Starting from a three-dimensional model, the method for determining the cavity-QED parameters (g , κ , γ) is presented, and the parameters are evaluated as functions of the input beam profile. It is shown that suppression of the radiative loss of cavity photons is possible by engineering the lateral profile of the input beam.

DOI: 10.1103/PhysRevA.73.053814

PACS number(s): 42.50.Pq, 42.50.Ct

I. INTRODUCTION

In cavity quantum electrodynamics (QED) systems, a well isolated system composed of atoms and cavity photons is coupled to the external photon field, which can be utilized as a probe for inferring the quantum state of atoms and cavity photons. Cavity QED systems are therefore suitable for fundamental tests of quantum dynamics in open systems and of their potential applications in quantum control technology [1,2]. In the strong-coupling regime of cavity QED, the atoms and the cavity mode exchange the energy quantum (Rabi flopping) [3,4] before it escapes out of the cavity. This internal dynamics is applied for preparation of nonclassical states, such as the number state of cavity photons [5,6] and the entangled states among atoms and cavity photons [7–9]. In combination with measurements on the probes, quantum nondemolition measurement of the cavity-photon number [10] and continuous monitoring of the atomic position inside the cavity [11,12] have been achieved. Besides isolation of the system, the cavity also plays a role of an amplifier of the input light field. Exploiting this magnification effect, significant nonlinear phase shift has been demonstrated by the weak field at the single-photon level [13,14]. The strong optical nonlinearity sensitive to individual photons [15–18], as well as the photon generation techniques [19–21], is the key ingredient for optical quantum computation [22,23]. Furthermore, combining the field magnification effect with multilevel quantum systems, electromagnetic-induced transparency (EIT) effects have been proved to occur at the few-photon level [24–26]. Recently, it was shown that the strong-coupling regime of cavity QED can be realized by solid-state systems, such as superconducting quantum circuits [27,28] and quantum dots [29,30], which will open new possibilities of cavity QED. Thus, the cavity QED plays a central role in the modern quantum control technology.

Another merit of cavity QED systems is that their dynamics can be analyzed precisely by a compact theoretical model with three principal parameters [1,31]: the atom-cavity dipole coupling g , the damping rate of the cavity mode κ , and the atomic decay rate into noncavity modes γ . In typical

cavity-QED experiments using real atoms, a cavity is formed by two spherical mirrors, where the spatial profile of the cavity mode is specified by geometric parameters such as the curvature of the mirrors and the cavity length [32,33]. In solid-state optical spectroscopy, optically active media are often confined in planar microcavities. When a planar cavity is used, the spatial profile of the input beam can be chosen more arbitrarily. In such systems, it is naturally expected that the cavity volume is determined not only by the geometric parameters of the cavity but also by the profile of the input beam (see Sec. II A). Therefore, the parameters g , κ , and γ would depend on, for example, the beam diameter and incident angle.

The purpose of the present study is to clarify theoretically how an “atom” (an effective two-level system such as a quantum dot) confined within a planar cavity behaves as a cavity QED system. Starting from a three-dimensional model of an atom-cavity system and an input beam, the prescription to determine the parameters g , κ , and γ is presented, and the parameters are evaluated as functions of the input beam diameter. It is revealed that the radiative loss of cavity photons can be vanished in principle with an appropriate choice of the lateral profile of the input beam. These theoretical results are expected to provide guiding principles for the design of a solid-state cavity QED systems with reduced radiative loss.

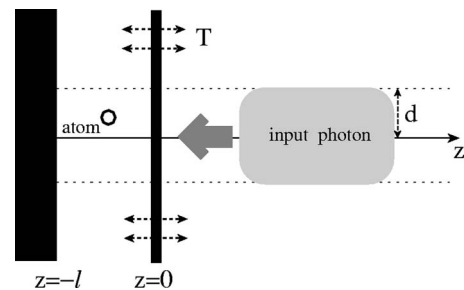


FIG. 1. Sketch of the system considered in this study. The planar cavity consists of a perfect mirror at $z = -l$ and a leaky mirror at $z = 0$. A two-level system (atom) is embedded in the cavity at $\mathbf{R} = (X, Y, Z)$ and a single photon is incident along the z axis with beam diameter $2d$.

*Electronic address: ikuzak@sys.wakayama-u.ac.jp

II. SYSTEM

The system considered in this study is illustrated in Fig. 1. A planar one-sided cavity is formed by a perfect mirror at $z=-l$ and a weakly transmissive mirror at $z=0$. The thickness of the leaky mirror is neglected here; the only parameter that characterizes the mirror is the transmissivity T . An atom with resonance frequency ω_a and transition dipole moment \wp is placed in the cavity at $\mathbf{R}=(X,Y,Z)$, where $-l<Z<0$. A single-photon state at normal incidence and fixed polarization is supplied as an input. The photon field can thus be treated simply as a scalar field. Assuming that the input beam diameter $2d$ is substantially larger than the diffraction limit, a separable wave function $\varphi(x,y)\psi(z)$, normalized as $\int dx dy |\varphi(x,y)|^2 = \int dz |\psi(z)|^2 = 1$, is employed for the input photon. The present discussion is restricted to the case of $\omega_a \approx \omega_c$, where $\omega_c = \pi/l$ is the cutoff frequency of the planar cavity ($\hbar=c=\epsilon_0=1$ throughout this study). In this case, only the lowest subband of the intracavity field ($k_z=\omega_c$) is relevant.

A. Estimation of g and κ

Intuitively, g and κ can be estimated as follows. The normalized cavity-mode function can be expressed as $f(\mathbf{r})=(2\omega_c/l\pi)^{1/2} \sin(\omega_c z)\varphi(x,y)$, assuming that the lateral profile is the same as that of the input beam. The atom-cavity coupling is therefore expected to have the form

$$g_{\text{est}} = \frac{\wp \omega_a}{\sqrt{2\omega_c}} f(\mathbf{R}) = \frac{\wp \omega_a}{\sqrt{\pi}} \sin(\omega_c Z) \varphi(X,Y), \quad (1)$$

where \wp denotes the transition dipole moment of the atom. From the transmissivity T of the mirror, the escape rate for cavity photons is expected to be

$$\kappa_{\text{est}} = T/2l = T\omega_c/2\pi. \quad (2)$$

The validity of these estimates will be examined later.

B. Three-dimensional formalism

Now we start to investigate the atom-photon interaction using a three-dimensional formalism. Denoting a two-dimensional in-plane wave vector (k_x, k_y) by \vec{k} and a three-dimensional wave vector (k_x, k_y, k_z) by \mathbf{k} , the Hamiltonian of this system is given by

$$\begin{aligned} \mathcal{H} = & \omega_a \sigma_+ \sigma_- + \int d^2 \vec{k} [\omega_{\vec{k}} c_{\vec{k}}^\dagger c_{\vec{k}} + (\lambda_{\vec{k}} \sigma_+ c_{\vec{k}} + \text{H.c.})] \\ & + \int d^3 \mathbf{k} \left[\omega_{\mathbf{k}} b_{\mathbf{k}}^\dagger b_{\mathbf{k}} + \left(\frac{c_{\vec{k}}^\dagger b_{\mathbf{k}}}{\sqrt{2\pi\tau_{\vec{k}}}} + \text{H.c.} \right) \right]. \end{aligned} \quad (3)$$

Here, σ_- , $c_{\vec{k}}$, and $b_{\mathbf{k}}$ are the annihilation operators for the atom, the intracavity field ($-l<z<0$), and the external field ($z>0$), respectively. It is of note that $c_{\vec{k}}$ has only two indices, since k_z is fixed at ω_c inside the cavity. The commutators for $c_{\vec{k}}$ and $b_{\mathbf{k}}$ are given by $[c_{\vec{k}}, c_{\vec{k}'}^\dagger] = \delta^2(\vec{k}-\vec{k}')$ and $[b_{\mathbf{k}}, b_{\mathbf{k}'}^\dagger] = \delta^3(\mathbf{k}-\mathbf{k}')$. $\omega_{\vec{k}}$ and $\omega_{\mathbf{k}}$ denote the energies for $c_{\vec{k}}$ and

$b_{\mathbf{k}}$, as given by $\omega_{\vec{k}} = (\omega_c^2 + |\vec{k}|^2)^{1/2}$ and $\omega_{\mathbf{k}} = |\mathbf{k}|$. The atom-photon coupling $\lambda_{\vec{k}}$ is given by

$$\lambda_{\vec{k}} = \frac{\wp \omega_a}{\sqrt{2\omega_{\vec{k}}}} f_{\vec{k}}(\mathbf{R}), \quad (4)$$

where $f_{\vec{k}}(\mathbf{r}) = \sqrt{\omega_c/2\pi^3} \sin(\omega_c z) \exp[i(k_x x + k_y y)]$ is the spatial mode function for $c_{\vec{k}}$. $\tau_{\vec{k}}$ is the lifetime of $c_{\vec{k}}$, as given by $\tau_{\vec{k}} = 2\pi\omega_{\vec{k}}/T\omega_c^2$. It is of note that the in-plane wave vector \vec{k} is conserved in the interaction between $c_{\vec{k}}$ and $b_{\mathbf{k}}$ due to translational symmetry. As quantum-dot systems have been shown to exhibit Fourier-transform-limited linewidths [20], the dephasing terms (e.g., the atom-phonon coupling) are neglected in the present treatment.

Although the input photon propagates in the $z>0$ region toward the negative z direction, it has been shown that the input photon may be regarded as propagating in the $z<0$ region toward the positive z direction [34]. Following this convention, the input photon state is given by

$$|\text{in}\rangle = \int d^3 \mathbf{r} \varphi(x,y) \psi(z) b_{\mathbf{r}}^\dagger |0\rangle, \quad (5)$$

where $|\psi(z)|^2$ is localized in the $z<0$ region and $b_{\mathbf{r}}$ is the Fourier transform of $b_{\mathbf{k}}$, that is, $b_{\mathbf{r}} = (2\pi)^{-3/2} \int d^3 \mathbf{k} e^{i\mathbf{k}\cdot\mathbf{r}} b_{\mathbf{k}}$.

III. EVALUATION OF CAVITY-QED PARAMETERS

A. Calculation of form factors

The objective is to derive, from Eqs. (3) and (5), the form factor $|\xi(\omega)|^2$ for overall atom-photon coupling and the form factor $|\xi_c(\omega)|^2$ for coupling to the quasicavity continuum [35]. To this end, the photonic part of the Hamiltonian is diagonalized, following the Fano method [36]. Approximating $\omega_{\mathbf{k}}$ by k_z , the eigenmode operator $B_{\vec{k}\omega}$ is given by

$$B_{\vec{k}\omega} = \alpha_{\vec{k}}(\omega) c_{\vec{k}} + \int dk_z \beta_{\vec{k}}(\omega, k_z) b_{\mathbf{k}}, \quad (6)$$

where

$$\alpha_{\vec{k}}(\omega) = \frac{(2\pi\tau_{\vec{k}})^{-1/2}}{\omega - \omega_{\vec{k}} + i/2\tau_{\vec{k}}}, \quad (7)$$

$$\beta_{\vec{k}}(\omega, k_z) = \frac{(2\pi\tau_{\vec{k}})^{-1}}{(\omega - \omega_{\vec{k}} + i/2\tau_{\vec{k}})(\omega - k_z + i\delta)} + \delta(\omega - k_z). \quad (8)$$

$B_{\vec{k}\omega}$ is normalized as $[B_{\vec{k}\omega}, B_{\vec{k}'\omega'}^\dagger] = \delta^2(\vec{k}-\vec{k}')\delta(\omega-\omega')$. Inversely, $c_{\vec{k}} = \int d\omega \alpha_{\vec{k}}^*(\omega) B_{\vec{k}\omega}$. Using $B_{\vec{k}\omega}$, the Hamiltonian can be rewritten as follows:

$$\mathcal{H} = \omega_a \sigma_+ \sigma_- + \int d^2 \vec{k} d\omega \{ [\lambda_{\vec{k}} \alpha_{\vec{k}}^*(\omega) \sigma_+ B_{\vec{k}\omega} + \text{H.c.}] + \omega B_{\vec{k}\omega}^\dagger B_{\vec{k}\omega} \}. \quad (9)$$

From this form of the Hamiltonian, it is straightforward to obtain the following expression for the overall form factor:

$$|\xi_t(\omega)|^2 = \int d^2\vec{k} |\lambda_{\vec{k}} \alpha_{\vec{k}}^*(\omega)|^2. \quad (10)$$

The overall form factor $|\xi_t(\omega)|^2$ is thus independent of the input photon profile, $\varphi(x, y)\psi(z)$. It can be readily confirmed that $|\xi_t(\omega)|^2$ is also independent of the in-plane position (X, Y) of the atom, as expected from the translational symmetry.

Next, we determine the quasicavity continuum. The input photon profile now becomes important at this stage. Denoting the Fourier transform of $\varphi(x, y)$ and $\psi(z)$ by $\tilde{\varphi}(\vec{k})$ and $\tilde{\psi}(k_z)$, and noting the fact that $\psi(z)$ is localized in the $z < 0$ region, the input state given by Eq. (5) can be rewritten as

$$|\text{in}\rangle = \int d^2\vec{k} d\omega \tilde{\psi}(\omega) \tilde{\varphi}(\vec{k}) \frac{\omega - \omega_{\vec{k}} - i/2\tau_{\vec{k}}}{\omega - \omega_{\vec{k}} + i/2\tau_{\vec{k}}} B_{\vec{k}\omega}^\dagger |0\rangle. \quad (11)$$

To relate the present problem to the conventional (g, κ, γ) model, the quasicavity continuum should be defined so as to contain the input photon state completely. Therefore, the quasicavity continuum C_ω is defined by

$$C_\omega^\dagger = \int d^2\vec{k} \tilde{\varphi}(\vec{k}) \frac{\omega - \omega_{\vec{k}} - i/2\tau_{\vec{k}}}{\omega - \omega_{\vec{k}} + i/2\tau_{\vec{k}}} B_{\vec{k}\omega}^\dagger. \quad (12)$$

Note that C_ω is normalized as $[C_\omega, C_{\omega'}^\dagger] = \delta(\omega - \omega')$. Thus, $|\xi_c(\omega)|^2$ is given by

$$|\xi_c(\omega)|^2 = |\langle 0 | \sigma_- \mathcal{H} C_\omega^\dagger | 0 \rangle|^2 = \left| \int d^2\vec{k} \tilde{\varphi}(\vec{k}) \lambda_{\vec{k}} \alpha_{\vec{k}}(\omega) \right|^2. \quad (13)$$

By the Schwartz inequality, $|\xi_c(\omega)|^2 \leq \int d^2\vec{k} |\tilde{\varphi}(\vec{k})|^2 \int d^2\vec{k} |\lambda_{\vec{k}} \alpha_{\vec{k}}(\omega)|^2 = |\xi_t(\omega)|^2$, which is in agreement with the present definitions. Thus, Eqs. (10) and (13) give the formal expressions for $|\xi_t(\omega)|^2$ and $|\xi_c(\omega)|^2$, respectively.

B. Relation between form factors and cavity-QED parameters

The relationship between the parameters (g, κ, γ) and the form factors $[|\xi_c(\omega)|^2$ and $|\xi_t(\omega)|^2]$ is as follows. In the conventional (g, κ, γ) model of cavity-QED, $|\xi_c(\omega)|^2$ is given by the Lorentzian

$$|\xi_c(\omega)|_{\text{con}}^2 = \frac{g^2 \kappa}{2\pi (\omega - \omega_c)^2 + \kappa^2/4}, \quad (14)$$

and $|\xi_t(\omega)|_{\text{con}}^2 = |\xi_c(\omega)|_{\text{con}}^2 + \gamma/2\pi$ [37]. Thus, the area of $|\xi_c(\omega)|^2$ corresponds to g^2 , i.e., $g^2 = \int d\omega |\xi_c(\omega)|^2$, while κ is identified as the half-width of $|\xi_c(\omega)|^2$. γ is dependent on the photon energy ω in general, although this ω dependence is usually neglected in the conventional (g, κ, γ) model. γ is given by $\gamma(\omega) = 2\pi[|\xi_t(\omega)|^2 - |\xi_c(\omega)|^2]$.

IV. NUMERICAL RESULTS

To embody these formal results, the discussion is restricted to the following case: (i) the lateral profile of

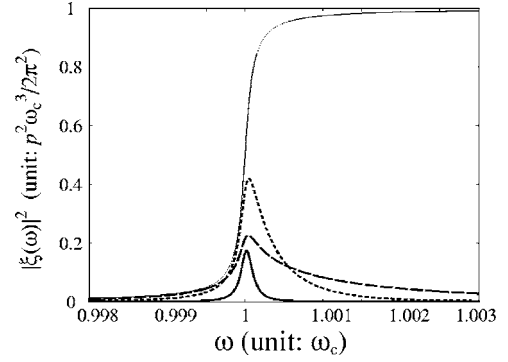


FIG. 2. Plot of $|\xi_t(\omega)|^2$ (thin line) and $|\xi_c(\omega)|^2$ (bold lines) for $d=20\omega_c^{-1}$ (dashed line), $50\omega_c^{-1}$ (dotted line), and $200\omega_c^{-1}$ (solid line). The transmissivity of the mirror is fixed at $T=10^{-3}$.

the input beam is Gaussian with diameter $2d$, i.e., $\varphi(x, y) = (\pi d^2)^{-1/2} \exp[-(x^2 + y^2)/2d^2]$, (ii) the atom is placed at the center of the cavity, i.e., $(X, Y, Z) = (0, 0, -l/2)$, (iii) the atom is resonant with the cavity, i.e., $\omega_a = \omega_c$.

A. Form factors

Figure 2 plots $|\xi_t(\omega)|^2$ and $|\xi_c(\omega)|^2$. Applying the approximation of $\tau_{\vec{k}} \approx \tau_0 = 2\pi/T\omega_c$ to Eq. (10), $|\xi_t(\omega)|^2$ is obtained analytically as

$$|\xi_t(\omega)|^2 = \frac{\varphi^2 \omega_c^3}{2\pi^2} \left[\frac{1}{2} + \frac{1}{\pi} \arctan\left(\frac{4\pi}{T\omega_c}(\omega - \omega_c)\right) \right], \quad (15)$$

which is in good agreement with the rigorous numerical result. The steplike behavior of $|\xi_t(\omega)|^2$ is a well-known property of the two-dimensional photon field [38].

In contrast to $|\xi_t(\omega)|^2$, which is determined solely by the transmissivity, $|\xi_c(\omega)|^2$ is also dependent on the beam diameter, as shown in Fig. 2. When d is large (solid line), $|\xi_c(\omega)|^2$ reduces to a genuine Lorentzian, expressed as Eq. (14) with $g = g_{\text{est}}$ and $\kappa = \kappa_{\text{est}}$. As d decreases, with a corresponding decrease in cavity volume, the atom-cavity coupling g increases and $|\xi_c(\omega)|^2$ becomes larger (dotted and dashed lines in Fig. 2). However, $|\xi_c(\omega)|^2$ cannot increase freely due to the upper bound imparted by the condition $|\xi_c(\omega)|^2 \leq |\xi_t(\omega)|^2$. This upper bound is expected to become important when d is sufficiently small to satisfy $\omega_c d \leq 4T^{-1/2}$, by comparing $|\xi_t(\omega)|^2$ [Eq. (15)] and $|\xi_c(\omega)|^2$ [Eq. (14) with Eqs. (1) and (2)] at $\omega = \omega_c$. It can be clearly seen in Fig. 2 that $|\xi_c(\omega)|^2$ deviates considerably from a genuine Lorentzian in the region of small d .

B. Evaluation of g and κ

The parameters g and κ can be evaluated from $|\xi_c(\omega)|^2$. Figure 3 plots g and κ as functions of the beam diameter $2d$ for three different values of T . The values of g and κ determined in the rigorous manner are in good agreement with the estimated values g_{est} and κ_{est} in the region of large d . However, in the region of small d satisfying $\omega_c d \leq 4T^{-1/2}$, the upper-bound condition $[|\xi_c(\omega)|^2 \leq |\xi_t(\omega)|^2]$ becomes se-

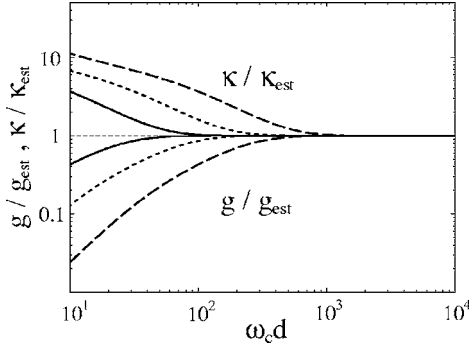


FIG. 3. Plot of g/g_{est} and $\kappa/\kappa_{\text{est}}$ as functions of beam diameter $2d$. g and κ are evaluated from $|\xi_c(\omega)|^2$, and g_{est} and κ_{est} are given by Eqs. (1) and (2). Plots are shown for transmissivities of $T=10^{-2}$ (solid lines), $T=10^{-3}$ (dotted lines), and $T=10^{-4}$ (dashed lines).

vere, and g and κ deviate appreciably from the estimated values.

C. Optimum beam profile for reduction of γ

It can be observed from Fig. 2 that $\gamma(\omega)$ is highly sensitive to ω in the present situation. Above the cutoff frequency, where the atom is allowed to emit photons in the in-plane direction, $\gamma(\omega)$ is large. In contrast, below the cutoff frequency, $|\xi_r(\omega)|^2$ is mostly occupied by $|\xi_c(\omega)|^2$, and $\gamma(\omega)$ is substantially suppressed. From the viewpoint of quantum control technology, this system becomes quite useful if $\gamma(\omega)$ can be reduced to zero, i.e., $|\xi_r(\omega)|^2 = |\xi_c(\omega)|^2$. In this case, the input photons with energy ω always appear in the output port after the interaction. That is, the system acts as a cavity-QED system without radiative loss. The Schwartz inequality suggests that $|\xi_r(\omega)|^2 = |\xi_c(\omega)|^2$ is achieved when $\tilde{\varphi}_{\text{lossless}}(\vec{k}; \omega) = |\xi_r(\omega)|^{-1} \lambda_{\vec{k}}^* \alpha_{\vec{k}}^*(\omega)$, where $|\xi_r(\omega)|^{-1}$ is a normalization factor. Thus, when the input photon energy is ω , lossless operation can be realized by choosing the lateral beam profile such that

$$\varphi_{\text{lossless}}(r; \omega) = \frac{1}{2\pi} \int d\vec{k} e^{i\vec{k}\cdot\vec{r}} \lambda_{\vec{k}}^* \alpha_{\vec{k}}^*(\omega), \quad (16)$$

where $\vec{r}=(x, y)$ and $r=|\vec{r}|$. The form of $\varphi_{\text{lossless}}(r; \omega)$ is plotted in Fig. 4. Below the cutoff frequency (bold lines in Fig. 4), $\varphi_{\text{lossless}}$ becomes a single-peaked and almost real function. Since $\varphi_{\text{lossless}}$ is not a genuine Gaussian, a perfectly lossless situation cannot be attained using a Gaussian beam. However, even with a Gaussian beam, the loss can be suppressed effectively if an appropriate beam diameter is chosen [$|\xi_c(\omega)|^2/|\xi_r(\omega)|^2 \sim 0.9$]. Above the cutoff frequency, $\varphi_{\text{lossless}}$ becomes an oscillatory complex function (thin lines in Fig. 4), which is far from Gaussian. Thus, the loss cannot be suppressed effectively above the cutoff frequency.

D. Realistic values of (g, κ, γ)

Here, we evaluate realistic values of (g, κ, γ) . We consider a situation in which the role of an “atom” is played by

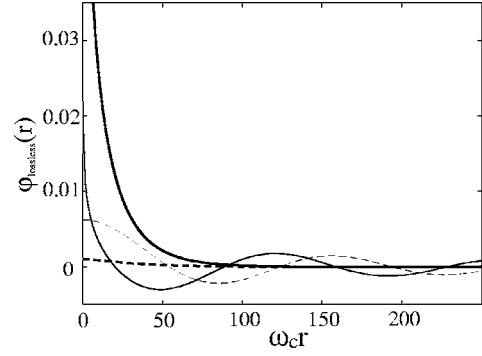


FIG. 4. Spatial form of $\varphi_{\text{lossless}}(r; \omega)$, showing real (solid lines) and imaginary (broken line) parts. The transmissivity T is 10^{-3} . Bold and thin lines denote results for $\omega/\omega_c=0.999$ and 1.001 , respectively.

a quantum dot with $\hbar\omega_a(=\hbar\omega_c)=1$ eV and a diameter of $a=10$ nm. The transition dipole moment φ of this dot is roughly given by $\varphi \approx qa$, where q is the electronic charge. The transmissivity T and beam diameter $2d$ are set at $T=10^{-3}$ and $d=50\omega_c^{-1} \approx 10 \mu\text{m}$ in reference to the dotted line in Fig. 2. In this case, $g/\omega_c \approx 6 \times 10^{-5}$ and $\kappa/\omega_c \approx 4 \times 10^{-4}$, and γ is most effectively suppressed at $\omega \approx 0.9998\omega_c$, where $\gamma/\omega_c \approx 7 \times 10^{-7}$.

Let us consider a case where an optimum two-photon pulse for maximizing nonlinearity (coherent length of 11 mm and central frequency of $0.9998\omega_c$) is inputted [37]. Then, the two-photon nonlinearity (the overlap between the output wave function and the *linear* output wave function) reaches -0.5 , which means that nonlinear sign shift in the output wave function is possible by the two-photon input. At the same time, the radiative loss of cavity photons into non-cavity modes is well suppressed (less than 1%). These values indicate the potential of this cavity QED system as a two-photon nonlinear device.

V. REMARKS

In the present study, a one-photon state [Eq. (5)] was selected as the input photon state. However, as the theory is constructed only by linear transformation on the photonic modes [Eqs. (6) and (12)], the results obtained here are also applicable to general input photonic states, such as the coherent state.

Limitations of the present treatment appear when extending consideration to beam diameters comparable to the photon wavelength, and to atomic resonances with higher harmonics of the cavity. That is, the use of a separable input wave function in Eq. (5) assumes that the beam diameter $2d$ is much larger than the wavelength ($\omega_c d \gg 1$). Discussion for much smaller values of d ($\omega_c d \sim 1$) will require the use of an inseparable input wave function. When the atom is resonant with higher harmonics of the cavity, i.e., $\omega_a \approx n\omega_c$ ($n \geq 2$), higher subbands of the intracavity field must be taken into account. However, both limitations appear relatively straightforward to resolve and will be examined in future work.

VI. SUMMARY

In summary, we have presented the theoretical prescription to determine the cavity-QED parameters (g, κ, γ) for an atom embedded in a planar cavity, starting from a three-dimensional formalism. The cavity-QED parameters can be evaluated through two kinds of form factors, namely the one for the overall atom-photon coupling and the one for coupling to the quasicavity continuum. The parameters depend on the lateral profile of the input beam. In particular, the system is shown to function as a cavity-QED system without

radiative loss of cavity photons ($\gamma=0$) under an adequate choice of the lateral beam profile.

ACKNOWLEDGMENTS

The author is grateful to Y. Shinozuka, H. Ishihara, K. Edamatsu, G. Oohata, and K. Miyajima for fruitful discussions. This research was partially supported by the following three grants: (i) the Research Foundation for Opto-Science and Technology, (ii) the Ministry of Education, Culture, Sports, Science and Technology, Grant-in-Aid for Young Scientists (B), No. 1774019, 2005, and (iii) Grant-in-Aid for Creative Scientific Research (17GS1204).

-
- [1] *Cavity Quantum Electrodynamics*, edited by P. R. Berman (Academic, San Diego, 1994).
- [2] H. Mabuchi and A. C. Doherty, *Science* **298**, 1372 (2002).
- [3] E. T. Jaynes and F. W. Cummings, *Proc. IEEE* **51**, 89 (1963).
- [4] G. Rempe, H. Walther, and N. Klein, *Phys. Rev. Lett.* **58**, 353 (1987).
- [5] B. T. H. Varcoe, S. Brattke, M. Weidinger, and H. Walther, *Nature (London)* **403**, 743 (2000).
- [6] S. Brattke, B. T. H. Varcoe, and H. Walther, *Phys. Rev. Lett.* **86**, 3534 (2001).
- [7] E. Hagley, X. Maitre, G. Nogues, C. Wunderlich, M. Brune, J. M. Raimond, and S. Haroche, *Phys. Rev. Lett.* **79**, 1 (1997).
- [8] A. Rauschenbeutel, G. Nogues, S. Osnaghi, P. Bertet, M. Brune, J. M. Raimond, and S. Haroche, *Science* **288**, 2024 (2000).
- [9] J. M. Raimond, M. Brune, and S. Haroche, *Rev. Mod. Phys.* **73**, 565 (2001).
- [10] G. Nogues, A. Rauschenbeutel, S. Osnaghi, M. Brune, J. M. Raimond, and S. Haroche, *Nature (London)* **400**, 239 (1999).
- [11] P. W. H. Pinkse, T. Fischer, P. Maunz, and G. Rempe, *Nature (London)* **404**, 365 (2000).
- [12] C. J. Hood, T. W. Lynn, A. C. Doherty, A. S. Parkins, and H. J. Kimble, *Science* **287**, 1447 (2000).
- [13] Q. A. Turchette, R. J. Thompson, and H. J. Kimble, *Appl. Phys. B* **60**, S1 (1995).
- [14] Q. A. Turchette, C. J. Hood, W. Lange, H. Mabuchi, and H. J. Kimble, *Phys. Rev. Lett.* **75**, 4710 (1995).
- [15] A. Gilchrist, G. J. Milburn, W. J. Munro, and K. Nemoto, e-print quant-ph/0305167.
- [16] W. J. Munro, K. Nemoto, and T. Spiller, *New J. Phys.* **7**, 137 (2005).
- [17] H. Jeong, *Phys. Rev. A* **72**, 034305 (2005).
- [18] J. H. Shapiro and R. S. Bondurant, *Phys. Rev. A* **73**, 022301 (2006).
- [19] P. G. Kwiat, K. Mattle, H. Weinfurter, A. Zeilinger, A. V. Sergienko, and Y. Shih, *Phys. Rev. Lett.* **75**, 4337 (1995).
- [20] C. Santori, D. Fattal, J. Vukovi, G. S. Solomon, and Y. Yamamoto, *Nature (London)* **419**, 594 (2002).
- [21] K. Edamatsu, G. Oohata, R. Shimizu, and T. Itoh, *Nature (London)* **431**, 167 (2004).
- [22] M. A. Nielsen and I. L. Chuang, *Quantum Computation and Quantum Information* (Cambridge Univ. Press, Cambridge, 2000).
- [23] E. Knill, R. Laflamme, and G. J. Milburn, *Nature (London)* **409**, 46 (2001).
- [24] M. Hennrich, T. Legero, A. Kuhn, and G. Rempe, *Phys. Rev. Lett.* **85**, 4872 (2000).
- [25] A. Kuhn, M. Hennrich, and G. Rempe, *Phys. Rev. Lett.* **89**, 067901 (2002).
- [26] M. Fleischhauer, A. Imamoglu, and J. P. Marangos, *Rev. Mod. Phys.* **77**, 633 (2005).
- [27] I. Chiorescu, P. Bertet, K. Semba, Y. Nakamura, C. J. P. M. Harmans, and J. E. Mooij, *Nature (London)* **431**, 159 (2004).
- [28] A. Wallraff, D. I. Schuster, A. Blais, L. Frunzio, R.-S. Huang, J. Majer, S. Kumar, S. M. Girvin, and R. J. Schoelkopf, *Nature (London)* **431**, 162 (2004).
- [29] J. P. Reithmaier, G. Sek, A. Löffler, C. Hofmann, S. Kuhn, S. Reitzenstein, L. V. Keldysh, V. D. Kulakovskii, T. L. Reinecke, and A. Forchel, *Nature (London)* **432**, 197 (2004).
- [30] T. Yoshie, A. Scherer, J. Hendrickson, G. Khitrova, H. M. Gibbs, G. Rupper, C. Ell, O. B. Shchekin, and D. G. Deppe, *Nature (London)* **432**, 200 (2004).
- [31] C. J. Hood, H. J. Kimble, and Jun Ye, *Phys. Rev. A* **64**, 033804 (2001).
- [32] G. D. Boyd and J. P. Gordon, *Bell Syst. Tech. J.* **40**, 489 (1961).
- [33] H. Kogelnik and T. Li, *Proc. IEEE* **54**, 1312 (1966).
- [34] H. F. Hofmann and G. Mahler, *Quantum Semiclass. Opt.* **7**, 489 (1995).
- [35] K. Koshino and A. Shimizu, *Phys. Rep.* **412**, 191 (2005).
- [36] U. Fano, *Phys. Rev.* **124**, 1866 (1961).
- [37] K. Koshino and H. Ishihara, *Phys. Rev. A* **70**, 013806 (2004); *Phys. Rev. Lett.* **93**, 173601 (2004).
- [38] H. Haug and S. W. Koch, *Quantum Theory of the Optical and Electronic Properties of Semiconductors* (World Scientific, Singapore, 1988).